

Automatic Parameterization of Force Fields for Liquids by Simplex Optimization

Roland Faller, Heiko Schmitz, Oliver Biermann,
Florian Müller-Plathe

Max-Planck Institut für Polymerforschung, Ackermannweg 10, D-55128 Mainz

November 26, 2024

Abstract We demonstrate an automatic method of force field development for molecular simulations. Parameter tuning is taken as an optimization problem in many dimensions. The parameters are automatically adapted to reproduce known experimental data such as the density and the heat of vaporization. Our method is more systematic than guessing parameters and, at the same time saves human labour in parameterization. It was successfully applied to several molecular liquids: As a test, force fields for 2-methylpentane, tetrahydrofurane, cyclohexene and cyclohexane were developed.

Keywords: force fields, molecular dynamics, parameter optimization, molecular liquids, simulation techniques

1 Introduction

In atomistic molecular dynamics simulations, one of the central problems is the choice of the proper parameters for modeling the desired system. There is a variety of approaches to this problem. Ab initio quantum chemistry would be an ideal tool for this purpose if it were able to handle interactions of big molecules in reasonable time. The standard solution, however, is quite pragmatic. One either chooses a force field that reproduces certain experimental data or one takes standard values for the different atoms. Hence, force field design is either a cumbersome trial-and-error procedure or relies heavily on the transferability of parameters.

There are attempts to make the computer do this job, e.g. force field development by weak coupling [1, 2]. However, that procedure relies on the requirements that one force field parameter dominates the behavior of one property and that their relationship is monotonic. As, in more complex force fields, one property may be influenced significantly by several parameters, a more general multidimensional optimization algorithm is needed. In our approach, we consider the experimentally measured properties as multi-dimensional functions of

the parameters. Then we use the well-known simplex algorithm [3] to find the optimum parameter set.

2 Algorithm and Implementation

2.1 Simplex algorithm

The simplex method is a well-known algorithm for minimization in many dimensions [3]. It is not constrained by conditions like monotonicity, convexity or differentiability of the function being optimized. It minimizes any single-valued function of an arbitrary number of variables. Additionally, it is very robust in finding a local optimum. Its main drawback is the large number of necessary function evaluations, i.e. in our case MD simulation runs, which are quite time consuming. In the following we briefly summarize the simplex algorithm used in this work.

A simplex (a “ d -dimensional distorted tetrahedron”) is a set of $d+1$ points in the d -dimensional parameter space. It is transformed geometrically depending upon the “quality” of the function values. There are three geometric transformations in the algorithm.

1. In a reflection, the point \mathbf{x}_i with the highest function value is reflected through the hyper-plane defined by the other points (see figure 1a).

$$\mathbf{x}'_i = \frac{2}{d} \sum_{j=1}^{d+1} \mathbf{x}_j - \left(\frac{2}{d} + 1 \right) \mathbf{x}_i \quad (1)$$

2. An expansion by the factor λ is a linear transformation of one point along the normal of the hyper-plane defined by the others (fig. 1b).

$$\mathbf{x}'_i = \frac{1-\lambda}{d} \sum_{j=1}^{d+1} \mathbf{x}_j - \left(\frac{1-\lambda}{d} + 1 \right) \mathbf{x}_i \quad (2)$$

Thus, a reflection is just the special case $\lambda = -1$.

3. A (d -dimensional) contraction is a linear transformation of all but one point \mathbf{x}_j towards the lowest point (fig. 1c). Contractions by a factor of 2 are applied.

$$\mathbf{x}'_i = \frac{1}{2}(\mathbf{x}_i + \mathbf{x}_j), \forall i \neq j \quad (3)$$

The algorithm runs iteratively. Each iteration starts with a reflection of the highest point. Depending on the function value at the new point, an expansion or a contraction is performed. If the new point is better than the best point an additional expansion with the factor $\lambda = 2$ (i.e. the distance to the hyper-plane of the others is doubled) is applied to explore further into this “promising”

direction. If the new point is very far away from the minimum (i.e. worse than the second worst point up to now) an expansion with $\lambda = 0.5$ is applied. If this resulting point is still very bad (in the above sense) a contraction around the best point is performed. Then the next iteration, starting again with a reflection, follows.

2.2 The target function evaluation

As the algorithm only knows about scalar functions in \mathcal{R}^d , we have to construct a single-valued function $f_{target}(p_1, \dots, p_d)$ of our force field parameters p_1, \dots, p_d . The function to be minimized should indicate the deviation of physical properties of the simulated model system from the real system as observed in experiments. Typically, one chooses a set of physical properties $\{P_i\}$, which are well characterized experimentally and converge rapidly in simulations. A natural choice for f_{target} is the square root of the weighted sum of relative squared deviations

$$f_{target}(\{p_n\}) = \left(\sum_i w_i \left(1 - \frac{P_i(\{p_n\})}{P_{i,target}} \right)^2 \right)^{1/2}, \quad (4)$$

where $P_{i,target}$ is the experimental value of property P_i . The square root is chosen because it comes steeper to the minimum. The weights w_i account for the fact that some property may be easier to reproduce than others. Thus, the algorithm can be forced to focus stronger on the difficult properties. Typically, the density ρ is easier reproduced than the enthalpy of vaporization ΔH_{vap} , which are the two properties we optimize our force fields against. They converge rapidly and experimental data is readily available for many fluids (see e.g. [4, 5]).

If the number of parameters to be optimized is about 2 to 4 the flexibility to fit the data is normally sufficient and the computational time is still manageable. If there are more target properties it may be necessary to increase the dimensionality of the optimization space at the cost of more computer time.

In the beginning, a simplex of parameter sets has to be constructed by the user. These data may be guessed from parameters for similar compounds or from standard force fields [6, 7, 8]. Furthermore, a starting configuration of the system is needed which should be close to the supposed real state. That means that geometry and density should be almost correct. The starting configuration is relaxed some picoseconds with a guessed force field in order to obtain a proper liquid structure. The target function for the initial parameter sets is first evaluated before the simplex algorithm starts.

2.3 Parameters to optimize

Since the dimensionality of parameter space is limited, we have to decide which parameters of the force field we want to optimize. This number is mainly limited by the available computing resources.

Typically, a Lennard-Jones potential is used to model the non-bonded interactions.

$$V_{LJ} = 4\epsilon \left(\left(\frac{\sigma}{r} \right)^{12} - \left(\frac{\sigma}{r} \right)^6 \right). \quad (5)$$

The density ρ depends quite strongly on the Lennard-Jones radius σ whereas the enthalpy of vaporization ΔH_{vap} depends stronger on ϵ . It is recommended to optimize non-bonded interaction parameters or charges and not the molecular geometry, because of simulational stability. The fact, that the geometry is mostly quite well known, supports this choice. There are several experimental methods to determine geometries, e.g. x-ray or neutron diffraction in the crystal or electron or microwave diffraction in the gas phase. Ab initio quantum chemistry, too, gives molecular structures with useful accuracy. These geometries can, in most cases, be used for the liquid phase as well. Hence, we did not try the algorithm on geometry optimization although this may be possible in principle. Our simulations focused on the liquid phase, whose macroscopic properties depend only weakly on internal force field parameters. Therefore, the force field parameters for angles and dihedral angles may be adopted from similar force fields.

2.4 Equilibration

A MD run can produce reliable results only if the system has been equilibrated. Therefore, we need a scheme to test for equilibration which has to fulfill several requirements: It has to reject reliably non-equilibrated configurations because otherwise all following results are meaningless. It has to work fully automatic inside the overall algorithm, and it has to equilibrate as fast as possible in order not to waste resources.

If the force field parameters (i.e. the Hamiltonian) of a simulation change between iterations, like in our case, a configuration equilibrated with respect to the old parameters is no longer equilibrated with respect to the new ones. Hence, after each change of parameters, i.e. in each step of the simplex algorithm we have to re-equilibrate with respect to the actual parameters. In order to do this, we take as the starting configuration the final configuration from a simulation with a parameter set, which is close to the new one. As “distance” in parameter space we define the sum of squared deviations

$$|\{p^{(new)}\} - \{p^{(old)}\}|^2 := \sum_{i=1}^n (p_i^{(new)} - p_i^{(old)})^2. \quad (6)$$

If, for some reason, the equilibration did not converge for that set or some other problem occurred a standard configuration is used.

Using the configuration selected in this way we start a number of successive equilibration runs (typical length 50ps with 1fs timestep). These runs are analyzed for equilibration until they are either accepted or a maximum number of

runs (in our case 10) is exceeded. In the latter case, the parameters are considered not useful and the target function f_{target} is set to an arbitrary high value in order to indicate the failure.

How does the automatic determination of equilibration work? To our knowledge, there is no strict criterion for equilibration. The standard procedure is to inspect visually the time development of a typical quantity (like the density for low molecular weight liquids). Then one decides if it “settled” to stochastic oscillations around a converged mean value. In our case, we use the following test: The time series of the density is cut into 3 to 5 intervals, for each of which the mean and the standard error are calculated. If all these averages agree within their errors the configuration is considered equilibrated. In comparison with the “human eye”-method, this method proved to be rather strict. However, this is necessary because we cannot accept non-equilibrated configurations which would mislead the simplex algorithm. The equilibration scheme worked well and led on average to an equilibrated configuration in about 3 to 4 runs. Naturally, the number of runs decreases during the optimization because the changes in the parameters get less drastic. We also checked a second equilibration test where the last third of the simulation was fitted by linear regression. If the slope is zero within its error the configuration is assumed equilibrated. The outcomes of the two tests differed only slightly.

Only very few parameter sets (less than 10%) had to be discarded due to non-equilibration. Even fewer led to instabilities in the simulation.

2.5 Convergence criterion

The simplex algorithm finishes if the target function falls below a given threshold l which is usually set to about 1% (i.e. $f_{target} < l \approx 0.01$). If this is achieved the parameters are deemed to be satisfactory. It does not make sense to reproduce experimental data more closely because the typical simulation error limits the reliability anyway. In addition, the target values themselves carry some uncertainty.

If the desired accuracy l is not achieved and the simplex ends up in a local minimum the algorithm is aborted. Therefore, the highest and lowest value of the target function in the actual simplex are compared. Hence, if

$$\max(f_{target}) - \min(f_{target}) < \delta f \approx 0.001 \quad (7)$$

is achieved further optimization makes no sense. In this case, either the number of parameters is too small to reproduce the desired number of properties (overdetermination) or the appropriate parameter values are far off the initial guess. We note that other convergence and abortion criteria are possible, for example based on the size of the simplex. However, ours have proven to work well in practice.

2.6 Implementation

The parts of the algorithm were implemented in different programming languages. The backbone is a *tcs*h script which calls all auxiliary programs and controls the overall flow of the procedure. It uses standard UNIX utilities like *awk*. The routine for producing a new topology from a set of parameters is a *PERL* script whereas the programs for calculating the distance in parameter space and the determination of equilibration are implemented in C++. Several programs from the *YASP* simulation package [9] are used: the MD program itself as well as the utilities for calculating enthalpy of vaporization and density. Any program or utility may be easily exchanged without affecting the overall structure, e. g. for using another MD program or a different equilibration scheme.

The structure of the procedure for obtaining a function value from a given set of parameters is shown in the flow diagram in figure 2.

3 Examples

The optimization procedure was tested with different model systems in order to explore its ability to produce force fields.

The all-atom nonbonded force field consists of a Lennard-Jones 12-6 potential and an electrostatic potential using reaction field and a finite cutoff (of 0.9nm)

$$V^{(nonb)} = 4\epsilon_{ij} \left(\left(\frac{\sigma_{ij}}{r} \right)^{12} - \left(\frac{\sigma_{ij}}{r} \right)^6 \right) + \frac{q_i q_j}{4\pi\epsilon_0\epsilon} \left(\frac{1}{r} + \frac{\epsilon_{RF} - 1}{2\epsilon_{RF} + 1} \frac{r^2}{r_{cutoff}^3} \right). \quad (8)$$

This potential is applied to atoms belonging to different molecules, internal non-bonded interactions are excluded in our test cases. The Lennard-Jones parameters between unlike atoms are derived by the Lorenz-Berthelot mixing rules [10]

$$\epsilon_{ij} = (\epsilon_{ii}\epsilon_{jj})^{\frac{1}{2}}, \quad \sigma_{ij} = \frac{1}{2}(\sigma_{ii} + \sigma_{jj}). \quad (9)$$

A bond angle potential

$$V^{(angle)} = \frac{k^{(angle)}}{2}(\Theta - \Theta_0)^2, \quad \Theta : \text{bond angle} \quad (10)$$

and, for some molecules, torsional potentials with threefold symmetry

$$V^{(tors)} = \frac{k^{(tors)}}{2}(1 - \cos(3\tau)), \quad \tau : \text{dihedral angle} \quad (11)$$

or a harmonic dihedral potential

$$V^{(hd)} = \frac{k^{(hd)}}{2}(\tau - \tau_0)^2 \quad (12)$$

are applied in order to keep the correct molecular shape.

The bond lengths were constrained using the SHAKE algorithm [11, 12]. Our systems are subject to cubic periodic boundary conditions. The simulations were run at ambient conditions ($T=298$ K, $p=1013$ hPa). The neighbor-list [10] is calculated up to 1.0nm every 10 to 15 time-steps. We use the Berendsen algorithm for constant pressure and temperature [13]. The coupling times were 0.2 ps and 2 ps, respectively. The simulation runs lasted 50 ps at a timestep of 1 fs for each equilibration run and 100 ps at a timestep of 2 fs for the evaluation runs. The errors of the properties were obtained by a binning analysis [10].

3.1 Methylpentane

As a first test, a system of 125 uncharged 2-methylpentane molecules was optimized with respect to density ρ and enthalpy of vaporization ΔH_{vap} . All Lennard-Jones parameters are subject to optimization. However, all like atoms (C and H) are constrained to have the same LJ parameters. The internal part of the force field is taken from the AMBER force field [6]. This comprises the rule that the Lennard Jones ϵ (eq. 5) is scaled by a factor of 0.5 for 1-4 interactions.

We used the following parameter file to start the algorithm. The number "4" in the second line indicates the dimensionality of the parameter space. The following five lines are the guesses of the parameters, the initial simplex. The last column shows the results after evaluation of the target function. The Lennard-Jones energies ϵ and ΔH_{vap} are measured in kJ/mol the radii σ in nm, the density ρ in kg/m³.

##	ϵ_C	σ_C	ϵ_H	σ_H	f_{target}	ΔH_{vap}	ρ
4							
0.291643	0.339215	0.154545	0.258859	0.030287	29.42	636.1	
0.290554	0.340351	0.151371	0.260571	0.052871	28.88	626.5	
0.290167	0.340656	0.151116	0.260825	0.057492	28.81	623.8	
0.290545	0.341183	0.149968	0.260762	0.043120	29.18	629.6	
0.290421	0.341161	0.150191	0.260763	0.051831	28.94	626.2	

These parameters produce properties which are already quite close to the target values. The simplex algorithm now does the fine tuning. First, the simplex is reflected away from parameter set 3. The new set is

##	ϵ_C	σ_C	ϵ_H	σ_H	f_{target}	ΔH_{vap}	ρ
0.291414	0.340299	0.151922	0.259653	0.045721	29.04	629.6	

After 11 optimization steps, which took about 2 weeks altogether on a DEC 433MHz processor, the optimization finally finished with the following values:

##	ϵ_C	σ_C	ϵ_H	σ_H	f_{target}	ΔH_{vap}	ρ
0.294477	0.336339	0.162144	0.254668	0.008629	30.15	652.7	

Figure 3 illustrates the progress of the optimization by means of a previous run. The circles in fig. 3a) show the results of function evaluations and the solid line

shows the current best values of f_{target} . In the beginning, the function values scatter quite strongly. In the run of the algorithm, this starts to decrease. Figure 3b) shows how density and enthalpy of vaporization reach their target values. The only maintenance which had to be done was restarting the algorithm after a shutdown of the computer system. The whole algorithm proved to be stable and worked fully automatically. Only once the equilibration failed due to exceeding the limit of 10 runs. It is shown by the spike in figure 3 (which goes up to 100000). The final force field is shown in table I. These values reproduced the experimental data in a satisfactory way (table II).

3.2 Tetrahydrofurane

As a different test system we used tetrahydrofurane (THF). Here, we especially focused on the optimization of partial charges. The hydrogens did not carry any partial charges but oxygen and carbon did. The charges of the carbons 2 and 5 and the carbons 3 and 4 are the same for symmetry reasons. With the constraint of electroneutrality, there were two charge parameters to be optimized. We chose q_O and $q_{C2/C5}$, then we have $q_{C3/C4} = \frac{1}{2}(-q_O - 2q_{C2/C5})$. Additionally, the oxygen parameters ϵ_O and σ_O were included in the optimization. The first guess for the partial charges was taken from a quantum chemical Hartree-Fock calculation with a 6-311G** basis set using Gaussian 94 (Mulliken charges with hydrogens summed into heavy atoms) [14]. This yielded also the bond angle values. The bond lengths are taken from electron diffraction [5]. The simulated system contained 216 molecules. The electrostatic interactions were simulated with a reaction field correction ($\epsilon_{RF} = 7.5$) using the same cutoff $r_c = 0.9$ nm as for the Lennard-Jones potential. Here the following starting simplex was taken:

##	$-q_O$	$q_{C2/C5}$	ϵ_O	σ_O	f_{target}	ΔH_{vap}	ρ
4							
0.581241	0.225443	0.516818	0.208594	0.084176	32.72	816.96	
0.658970	0.251733	0.325788	0.300391	0.137257	35.39	811.81	
0.480765	0.251793	0.635725	0.316797	0.186735	27.68	774.02	
0.684265	0.276431	0.729962	0.264345	0.232852	39.29	847.92	
0.582970	0.220928	0.535152	0.192715	0.088840	33.57	823.39	

The first optimization attempt, which tried to optimize procedure the above parameters, ended up in a local minimum with $f_{target} \approx 0.07$ after 53 evaluations because the experimental liquid density could not be reproduced satisfactorily. It was systematically too low. Therefore, the best parameters so far were frozen and a new optimization was started where only the Lennard-Jones radii of all species were optimized. Finally, convergence ($f_{target} \leq 0.01$) was achieved. The resulting THF force field is described in table III.

These parameters lead to the physical properties shown in table IV. Our force field has about the same accuracy as an earlier Monte Carlo simulation of a united atom OPLS model for THF [15].

3.3 Cyclic Hydrocarbons

Finally, the method was applied in order to obtain force fields for cyclohexene and cyclohexane with 125 molecules in the periodic box. The geometries were taken from electron diffraction data [5]. The geometric data are shown in table V. In the cyclohexene force field, harmonic dihedral angles are used in order to keep the atoms around the double bond in plane, since the sp^2 hybridisation prevents the double bond from rotating. Additionally, standard torsional potentials with three-fold symmetry are used. Cyclohexane was simulated without any dihedral angle potentials. For the angular force constants we used a standard value, since they are believed to be of minor importance for the desired properties. Additionally, they may be compensated by the nonbonded parameters.

The optimized Lennard-Jones 12-6 parameters are shown in table VI. The parameters included in the optimization procedure are denoted with *opt* in the table. No charges were used. All the parameters which are not optimized as well as the initial simplices have been taken from similar force fields.

Except for the Lennard-Jones ϵ of the hydrogens, the resulting final parameters are very similar for the two molecules. This shows that force field parameters are not a unique description of a certain atom type but rather they are only a part of the overall molecular description. Mostly, however, the same atoms in similar environments may be described by similar parameters.

We compare our thermodynamic data with experiment in table VII. A more detailed analysis of transport properties of these cyclic hydrocarbons will be published elsewhere [16]. The cyclohexane force field yields a slightly better comparison to experiment than in a recent study using a commercial force field [8] whereas the study of cyclohexene is the first to our knowledge.

4 Conclusions

We applied the simplex algorithm to the problem of force field optimization for MD simulations. Given a good initial guess for the force field parameters and the experimental data for some properties, our method tunes the parameters to optimum values. Once the routine has been set up, very little human interference is required for maintenance. The algorithm proved to be robust and found local minima if set up properly. The resulting force fields are able to reproduce experimental data of low molecular weight liquids in a satisfactory way.

In the examples of this contribution, we typically optimized 4 force field parameters against 2 observables. Hence, the solutions are most likely not unique. This, however, is a feature of the problem of finding a force field given a small number of observables, not of the algorithmic solution presented here. Density and enthalpy of vaporization are the two properties most commonly used to derive force fields, as they are experimentally available for many fluids and quickly converging in a simulation. At present, our method has to be used with a judicious choice of starting values for the parameters to prevent it

from optimizing towards an unphysical, non-transferable set of parameters. It shares this restriction with all other methods of finding force fields, including “optimization by hand”. On the other hand, it is mostly not difficult to come up with a reasonable first guess for the parameters. What is time consuming is the fine tuning and it is at this point where our method offers help.

A possible way out of the dilemma is to increase the base of experimental observables used in the target function. In a few selected cases we have used other liquid properties than ρ and ΔH_{vap} together with the other refinement scheme [1, 2]. However, one has to note that there are not too many suitable fluid properties. Some properties are of similar character to what we already have. For example, the excess chemical potential μ_{ex} probes almost the same regions of the force field as ΔH_{vap} and, thus, does not add much independent information. Dynamic properties often converge too slowly in simulations to be useful (shear viscosity, dielectric constant) or the experimental data are not of sufficient quality (tracer diffusion coefficient, molecular reorientation times). We, therefore, follow the strategy of optimizing towards ρ and ΔH_{vap} and subsequently checking the final force field against other liquid properties. For our models of cyclic hydrocarbons we have, for instance, calculated tracer and binary diffusion coefficients as well as molecular reorientation times for both the pure liquids and binary mixtures, and the results agree well with experimental data where available [16].

The automatic parameterization scheme presented has the small disadvantage of probably requiring moderately more computer time than an optimization by hand. This is more than offset by the invaluable advantage of freeing researchers from the labour of parameter optimization. In a reasonable use of computing time (a few weeks workstation time) one is able to cope with dimensionalities of parameter space of about 4. This depends, however, strongly on the actual simulations to be performed. On the other hand, the full potential of speeding up our algorithm has not yet been realized. We foresee possibilities of substantial improvement by using a less rigorous and maybe adaptive equilibration scheme and by substituting the simplex algorithm by a faster converging optimizer (e.g. Fletcher) in the final stages of minimization. This remains an interesting starting point for future research.

References

- [1] Njo, S. L.; van Gunsteren, W. F.; Müller-Plathe, F. *J Chem Phys* 1995, 102, 6199–6207.
- [2] Berweger, C. D.; van Gunsteren, W. F.; Müller-Plathe, F. *Chem Phys Letters* 1995, 232, 429–436.
- [3] Press, W. H.; Teukolsky, S. A.; Vetterling, W. T.; Flannery, B. P. *Numerical Recipes in C: The Art of Scientific Computing*; Cambridge University Press: New York, second edition 1992.

- [4] Landolt, H.; Börnstein Numerical data and functional relationships in science and technology; Springer: Berlin, 1993.
- [5] Lide, D. R., ed. CRC handbook of chemistry and physics; CRC Press: Boca Raton, 76th edition 1995.
- [6] Cornell, W. D.; Cieplak, P.; Bayly, C. I.; Gould, I. R.; Merz Jr., K. M.; Ferguson, D. M.; Spellmeyer, C. D.; Fox, T.; Caldwell, J. W.; Kollman, P. A. *J Am Chem Soc* 1995, 117, 5179–5197.
- [7] van Gunsteren, W. F.; Billeter, S. R.; Eising, A. A.; Hünenberger, P. H.; Krüger, P.; Mark, A. E.; Scott, W. R. P.; Tironi, I. G. *Biomolecular simulation: The GROMOS manual and user guide*; Vdf: Zürich, 1996.
- [8] Sun, H. *J Phys Chem B* 1998, 102, 7338–7364.
- [9] Müller-Plathe, F. *Comput Phys Commun* 1993, 78, 77–94.
- [10] Allen, M. P.; Tildesley, D. J. *Computer Simulation of Liquids*; Clarendon Press: Oxford, 1987.
- [11] Ryckaert, J.-P.; Cicotti, G.; Berendsen, H. J. C. *J Comput Phys* 1977, 23, 327–341.
- [12] Müller-Plathe, F.; Brown, D. *Comput Phys Commun* 1991, 64, 7–14.
- [13] Berendsen, H. J. C.; Postma, J.; van Gunsteren, W.; DiNola, A.; Haak, J. *J Chem Phys* 1984, 81, 3684–3690.
- [14] Frisch, M. J.; Trucks, G. W.; Schlegel, H. B.; Gill, P. M. W.; Johnson, B. G.; Robb, M. A.; Cheeseman, J. R.; Keith, T. A.; Petersson, G. A.; Montgomery, J. A.; Raghavachari, K.; Al-Laham, M. A.; Zakrzewski, V. G.; Ortiz, J. V.; Foresman, J. B.; Cioslowski, J.; Stefanov, B. B.; Nanayakkara, A.; Challacombe, M.; Peng, C. Y.; Ayala, P. Y.; Chen, W.; Wong, M. W.; Andres, J. L.; Replogle, E. S.; Gomperts, R.; Martin, R. L.; Fox, D. J.; Binkley, J. S.; Defrees, D. J.; Baker, J.; Stewart, J. P.; Head-Gordon, M.; Gonzalez, C.; Pople, J. A. *Gaussian 94*; Gaussian, Inc.: Pittsburg PA, 1995.
- [15] Briggs, J. M.; Matsui, T.; Jorgensen, W. L. *J Comput Chem* 1990, 11, 958–971.
- [16] Schmitz, H.; Faller, R.; Müller-Plathe, F. *Molecular mobility in cyclic hydrocarbons - a simulation study* *J. Phys. Chem. B*, submitted.
- [17] Harris, K. R.; Dunlop, P. J. *Ber Bunsenges Phys Chem* 1994, 98, 560–562.

bonded parameters		non-bonded parameters	
parameter	value	parameter	value
C-C	0.1526 nm	m_C	12.01 amu
C-H	0.109 nm	m_H	1.00782 amu
$k_{C-C-C}^{(angle)}$	$167.47 \frac{\text{kJ}}{\text{mol rad}^2}$	ϵ_C	0.294 kJ/mol
$k_{C-C-H}^{(angle)}$	$209.34 \frac{\text{kJ}}{\text{mol rad}^2}$	ϵ_H	0.162 kJ/mol
$k_{H-C-H}^{(angle)}$	$146.54 \frac{\text{kJ}}{\text{mol rad}^2}$	σ_C	0.336 nm
H-C-H	109.5°	σ_H	0.254 nm
C-C-C	109.5°		
C-C-H	109.5°		
$k_{C-C-C-C}^{(tors)}$	11.5kJ/mol		
$k_{methyl}^{(tors)}$	11.5kJ/mol		

Table I: Details of the Methylpentane force field

	exp.	sim.
ΔH_{vap} [kJ/mol]	29.89[5]	29.92±0.03
ρ [kg/m ³]	653.0[5]	653.4±0.5
D [cm ² /s]		$(2.5\pm 0.2)\times 10^{-5}$

Table II: Experimental and simulated properties of 2-methylpentane

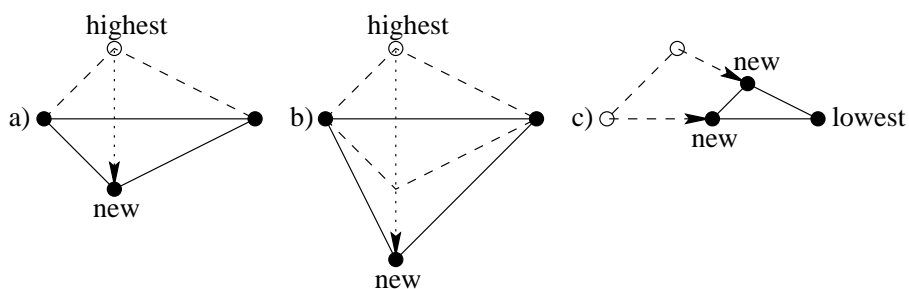


Figure 1: Transformations of the simplex used during the algorithm: a) reflection, b) expansion, c) contraction.

nonbonded parameters		bonded parameters	
parameter	value	parameter	value
ϵ_{O}	0.509 kJ/mol	C-O	0.1428 nm
ϵ_{H}	0.200 kJ/mol	C-H	0.1115 nm
ϵ_{C}	0.290 kJ/mol	C-C	0.1536 nm
σ_{O}	0.243 nm	$k^{(angle)}$	$450.0 \frac{\text{kJ}}{\text{mol rad}^2}$
σ_{H}	0.193 nm	C-O-C	111.2°
σ_{C}	0.306 nm	O-C-C	106.1°
q_{O}	-0.577 e	C-C-C	101.4°
$q_{\text{C}2}$	0.228 e	O-C-H	109.0°, 109.3°
$q_{\text{C}3}$	0.061 e	C ₃ -C ₂ -H	111.0°, 113.2°
m_{O}	15.9949 u	H-C ₂ -H	108.2°
m_{C}	12.0 u	H-C ₃ -H	108.1°
m_{H}	1.00787 u	C ₂ -C ₃ -H	110.4° (2×)
			112.8° (2×)
		C ₃ -C ₄ -H	113.7° (2×)
			110.4° (2×)

Table III: Optimized force field for tetrahydrofurane. In the case of two angles in one line one is applied to the first hydrogen, the other to the second hydrogen, otherwise the angles would not be consistent with each other.

	experiment[5]	simulation (this work)	simulation [15]
ρ	889.0 kg/m ³	(886.0 ± 1.3) kg/m ³	(882±1) kg/m ³
ΔH_{vap}	31.99 kJ/mol	(32.0±0.1) kJ/mol	(31.57±0.08) kJ/mol

Table IV: Properties of tetrahydrofurane

property	C ₆ H ₁₀	C ₆ H ₁₂
$ C_{sp2}=C_{sp2} $	0.1334nm	
$ C_{sp2}-C_{sp3} $	0.150nm	
$ C_3-C_4 , C_5-C_6 $	0.152nm	
$ C_4-C_5 $	0.154nm	
$ C-C $		0.1526nm
$ C_{sp2}-H $	0.108nm	
$ C_{sp3}-H $		0.109nm
$k_{C-C-C}^{(angle)}$	$450 \frac{\text{kJ}}{\text{mol rad}^2}$	$335 \frac{\text{kJ}}{\text{mol rad}^2}$
$k_{C=C-C}^{(angle)}$	$500 \frac{\text{kJ}}{\text{mol rad}^2}$	
$k_{C-C-H}^{(angle)}$	$500 \frac{\text{kJ}}{\text{mol rad}^2}$	$420 \frac{\text{kJ}}{\text{mol rad}^2}$
$k_{H-C-H}^{(angle)}$	$500 \frac{\text{kJ}}{\text{mol rad}^2}$	$290 \frac{\text{kJ}}{\text{mol rad}^2}$
C=C-C	112.0°	
C-C-C	110.9°	109.5°
C _{sp2} -C-C	123.45°	
C-C-H		109.5°
C-C _{sp2} -H	119.75°	
H-C-H		109.5°
$k_{C-C=C-C}^{(hd)}$	$250 \frac{\text{kJ}}{\text{mol rad}^2}$	
$k_{H-C=C-C}^{(hd)}$	$200 \frac{\text{kJ}}{\text{mol rad}^2}$	
$k_{C-C-C-C}^{(tors)}$	10kJ/mol	

Table V: Geometry of the cyclic hydrocarbons and their intramolecular potentials

parameter	opt/fix	C ₆ H ₁₀	C ₆ H ₁₂
ϵ_C	opt	0.296kJ/mol	0.299kJ/mol
ϵ_H	opt	0.265kJ/mol	0.189kJ/mol
σ_H	opt	0.252nm	0.258nm
σ_C	opt		0.328nm
$\sigma_{C_{sp2}}$	fix	0.321nm	
$\sigma_{C_{sp3}}$	fix	0.311nm	
m_C	fix	12.01amu	
m_H	fix	1.00787amu	

Table VI: Cyclohexene and cyclohexane non-bonded parameters

	cyclohexene		cyclohexane		
	exp	sim	exp[5]	sim (this work)	sim [8]
ρ [kg/m ³]	805.8 [17]	806.0 \pm 1.5	777.6	775.9 \pm 0.8	774 \pm 2
ΔH_{vap} [kJ/mol]	33.47 [5]	33.3 \pm 0.1	33.33	33.46 \pm 0.05	33.41

Table VII: Properties of cyclohexene and cyclohexane

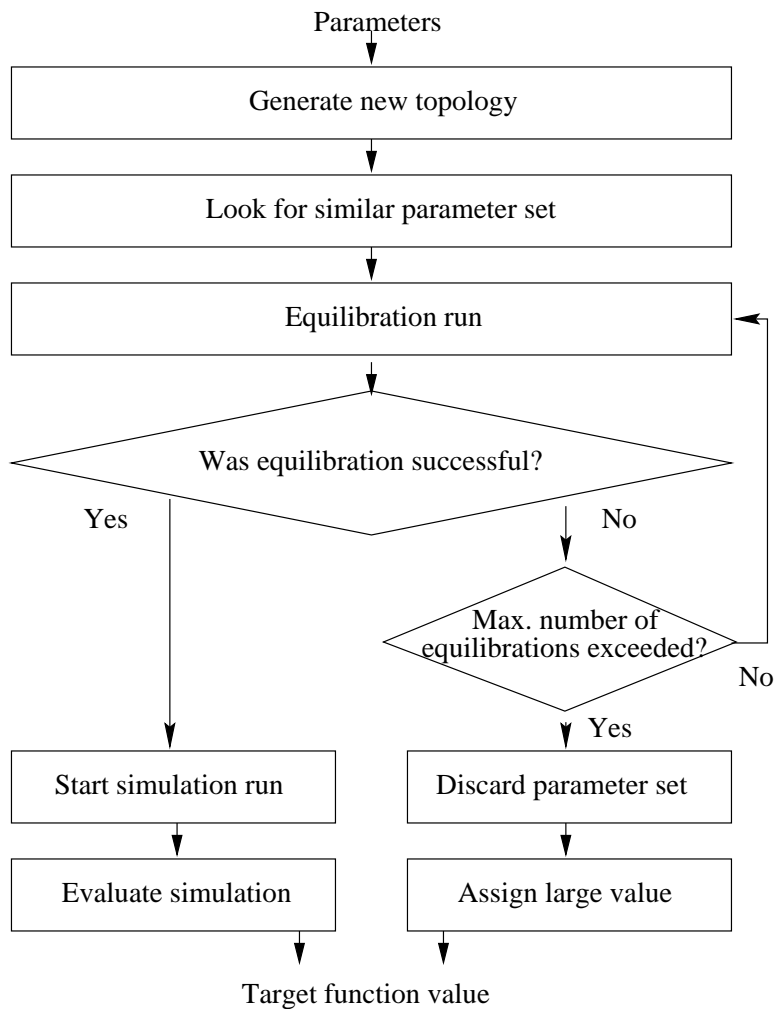


Figure 2: Flow diagram of the algorithm, one iteration.

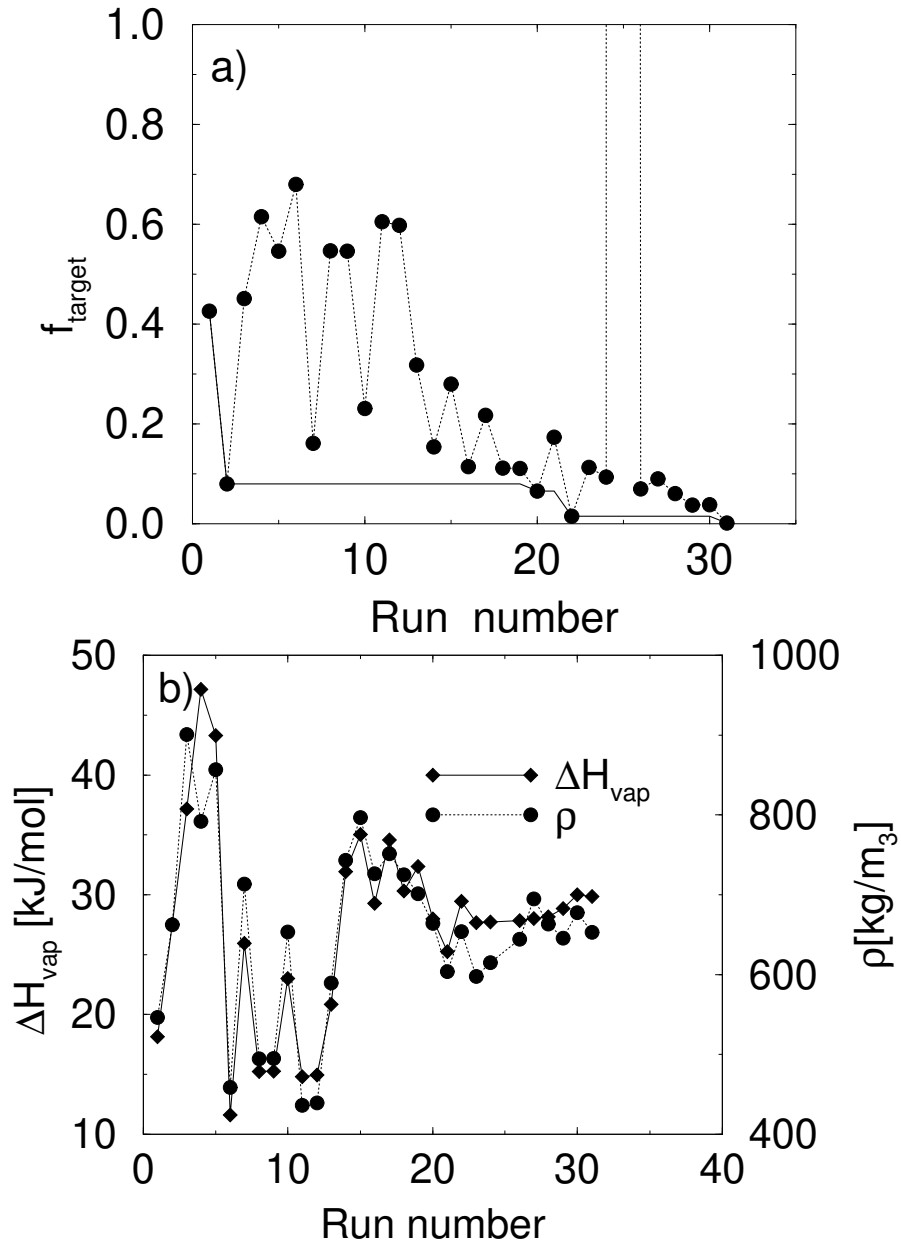


Figure 3: Convergence of a previous methylpentane optimization run: a) Target function: Solid line: best value of f_{target} ; Circles/dotted line: actual value of f_{target} . b) Properties: density and enthalpy of vaporization.